

Article

Electronically Stabilized Copoly(Styrene-Acrylic Acid) Submicrocapsules Prepared by Miniemulsion Copolymerization

Minkwan Kim, Yura Hwang and Han Do Ghim *

Department of Textile System Engineering, Kyungpook National University, 80 Daehakro, Bukgu, Daegu 41566, Korea; gundamzxv@naver.com (M.K.); youra3670@naver.com (Y.H.)

* Correspondence: hdghim@knu.ac.kr; Tel.: +82-53-950-7581

Academic Editor: Chris Fellows

Received: 1 July 2017; Accepted: 20 July 2017; Published: 20 July 2017

Abstract: This work reports the preparation and characterization of poly(styrene-acrylic acid) (St/AA) submicrocapsules by using the miniemulsion copolymerization method. AA was introduced to miniemulsion polymerization of St to increase the zeta potential and the resulting electrostatic stability of St/AA submicrocapsules. Phytoncide oil was adopted as the core model material. Miniemulsion copolymerization of St and AA was conducted at a fixed monomer concentration (0.172 mol) with a varying monomer feed ratio [AA]/[St] (0.2, 0.25, 0.33, 0.5, and 1.0). Concentrations of initiator (azobisisobutyronitrile; 1.0×10^{-3} , 2.0×10^{-3} , 3.0×10^{-3} , and 4.0×10^{-3} mol/mol of monomer) and surfactant (sodium dodecyl sulfate; 0.6×10^{-3} , 1.0×10^{-3} , and 1.4×10^{-3} mol) were also controlled to optimize the miniemulsion copolymerization of St and AA. Dynamic light scattering and microscopic analyses confirmed the optimum condition of miniemulsion copolymerization of St and AA. Long-term colloidal stability of aqueous St/AA submicrocapsule suspension was evaluated by using Turbiscan™ Lab. In this work, the optimum condition for miniemulsion copolymerization of St and AA was determined ([AA]/[St] = 0.33; [SDS] = 1.0×10^{-3} mol; [AIBN] = 2.0×10^{-3} mol/mol of monomer). St/AA submicrocapsules prepared at the optimum condition (392.6 nm and -55.2 mV of mean particle size and zeta potential, respectively) showed almost no variations in backscattering intensity (stable colloids without aggregation).

Keywords: styrene; acrylic acid; submicrocapsule; miniemulsion copolymerization; zeta potential

1. Introduction

Deliveries of functional hydrophobic materials using polymeric nanoparticles have been of great interest in biomedical sciences [1–6]. Furthermore, emulsions containing polymers can be applied to modify the surface of porous materials, endowing hydrophobic characteristics [7–9].

There are many methodologies for preparing nanoparticles including miniemulsion polymerization [10–13], interfacial polymerization, solvent evaporation, solvent deposition, nanoprecipitation, desolvation of natural polymers [14], and emulsification–diffusion [15–17]. Among these methods, miniemulsion polymerization is conducted by adopting cosurfactants such as hexadecane, cetyl alcohol, and so on. The existence of surfactant and cosurfactant ensures the formation of stable o/w miniemulsion (or nanoemulsion) under high shear without coalescence and Ostwald ripening [18]. Unfortunately, however, resulting nanoparticles and submicroparticles show insufficient dispersibility because of particle coagulation due to a lack of surface charge.

Zeta potential is the potential difference between the dispersion medium (water, in this case) and the stationary layer of fluid attached to the dispersed particle [19]. Therefore, the zeta potential can be used as a key indicator of the stability of colloidal dispersions because the magnitude of the

zeta potential indicates the degree of electrostatic repulsion between particles in a dispersion. For small particles, high zeta potential will confirm the electrostatic stability, preventing aggregation in the dispersion. If the zeta potential is small, this electrostatic repulsion may not be implemented by exceeding attractive forces, resulting in the flocculation of particles. Mandzy et al. [20] reported that reagglomeration of the TiO₂ nanoparticle dispersion could be prevented by electrostatic stabilization when its zeta potential value was less than -30 mV or greater than $+30$ mV. Many other researchers have investigated the effects of zeta potential on particle stability for metallic powders including zirconia and titania [21–24].

Polystyrene nanocapsules have been adopted as vehicles for photochromophores [25], phase change materials [26], and so on, by virtue of their ease of preparation and thermal stability. However, chronic particle aggregation of polystyrene nanoparticles has constrained their practical usage. Even though several researchers have investigated the miniemulsion polymerization of styrene (St) and acrylic acid (AA) to enhance the colloidal stability of polystyrene nanocapsules, copolymerization of AA and St with over 20 wt % of AA has rarely been considered for water compatibility of AA [27–29]. In this work, we adopted AA to miniemulsion polymerization of St to increase the zeta potential and resulting electrostatic stability of St/AA submicrocapsules containing phytoncide oil. To this aim, St/AA submicrocapsules were prepared at over 20 wt % of AA content. Mean particle size and zeta potential of St/AA submicrocapsules were then analyzed by dynamic light scattering (DSL). Dispersability of submicrocapsules was also evaluated by Turbiscan™ Lab to confirm the sink stability over time.

2. Materials and Methods

2.1. Materials

St and AA were purchased from Aldrich Chemical (St. Louis, MI, USA) and used as monomers after distillation. Azobisisobutyronitrile (AIBN) and divinyl benzene (DVB) were also provided by Aldrich Chemical (St. Louis, MI, USA) and used as initiator and crosslinking agent, respectively. Dae Jung Chemical (Siheung, Korea) supplied sodium dodecyl sulfate (SDS), which is used as surfactant. *n*-Hexadecane was purchased from Alfa Aesar (Ward Hill, MA, USA) and used as cosurfactant. Distilled water was of Milli-Q quality (Millipore, Billerica, MA, USA). Phytoncide oil was provided by CNG Co. (Daegu, Korea). All the reagents were of either HPLC grade or American Chemical Society analytical grade.

2.2. Miniemulsion Copolymerization

SDS ($0.6\text{--}1.4 \times 10^{-3}$ mol) was dissolved in distilled water to prepare the water phase. St and AA were homogeneously mixed with phytoncide oil, and *n*-hexadecane to form the oil phase. These solutions were emulsified with homogenizer for 10 min at 19,000 rpm to prepare micelles in submicrometer range. AIBN (initiator, $1.0\text{--}4.0 \times 10^{-3}$ mol/mol of monomer) was added at 60 °C and copolymerization was maintained for 6 h. The pH of the reaction system was slightly lowered with the increase of the amount of AA, ranging from 2.3 to 2.6. Detailed experimental conditions are presented in Table 1.

Table 1. Experimental conditions for miniemulsion copolymerization of St and AA.

Phase	Ingredients	Condition
Water phase	Distilled water	80 mL
	SDS	$0.6\sim 1.4 \times 10^{-3}$ mol
Oil phase	Phytoncide oil	10 g
	DVB	250 mg
	<i>n</i> -Hexadecane	450 mg
	Monomer	0.172 mol
	(feed ratio [AA]/[St])	(0.2~1.0)
Homogenization	Rate	19,000 rpm
	Duration	10 min

2.3. Characterization

The size and morphology of St/AA submicrocapsules were analyzed by scanning electron microscopy (SEM) (SU8220, Hitachi, Tokyo, Japan). The mean particle diameters and zeta potentials of St/AA submicrocapsules were also determined using DLS (ELS8000, Photal Otsuka Electronics, Osaka, Japan) equipped with vertically polarized light supplied by a He-Ne laser, operated at 10 mW. DLS measurements were performed at room temperature. The dispersion stability of St/AA submicroparticles in the aqueous phase was evaluated from the time variation of backscattered light by using the TurbiscanTM Lab (Formulation LAB, Toulouse, France). All the measurements were repeated three times.

3. Results and Discussion

3.1. Effects of Monomer Feed Ratio

The aim of miniemulsion copolymerization of St and AA is to increase the stability and prevent the coagulation of submicrocapsules containing functional materials in the core (phytoncide oil, in this case) by virtue of the enhanced zeta potential of submicrocapsules due to $-\text{COO}^-$ functional groups of AA. The salient feature of our current study is that miniemulsion copolymerization of St with AA yields electronically stabilized submicrocapsules which can be used as carriers for the lyophobic core.

Figure 1 shows the effects of the monomer feed ratio [AA]/[St] of miniemulsion copolymerization of St and AA on the mean particle size and zeta potential of the St/AA submicrocapsule. The particle size of the St/AA submicroparticle presents a minimum value of 392.6 nm at 0.33 of the monomer feed ratio (Figure 1a). The particle size of the St/AA submicroparticles decreased with the increase of [AA] at [AA]/[St] = 0.2~0.33 range, which was ascribed to the increased surface potential of micelles. For increased [AA]/[St] over 0.33, however, there was a steep increase in the mean particle size of the submicroparticles. As is well known, copolymerization behavior is mainly affected by the different reactivities of monomers. Compared with St, AA polymerizes vary rapidly, especially at low pH. Therefore, the increase of AA led inevitably to longer polyacrylic blocks in the copolymer formation at the particle–water interface, and increased the particle diameter. The increase in particle size with the increase in the amount of AA results in the formation of a hydrophilic swollen layer around the particle [27]. Absolute value of zeta potential (Figure 1b) increased to -55.2 mV with the increases of [AA] at [AA]/[St] = 0.2~0.33 range. The decrease in the absolute zeta potential value at over [AA]/[St] = 0.33 was attributed to the particle agglomeration in the aqueous phase due to the increased hydrophilic swollen layer of the particles and resulting reduction in surface area [29,30]. This can also be confirmed from SEM photographs presented in Figure 2. The St/AA submicroparticles prepared at [AA]/[St] = 0.5 and 1.0 showed crumpled and contorted morphology, which arose from the agglomeration of particles due to the fusion of hydrophilic swollen layers in dispersive medium.

Fused morphology of St/AA submicrocapsules indicates the low thermal durability of the wall of submicrocapsules that is unable to tolerate the deposition process prior to microscopic analysis.

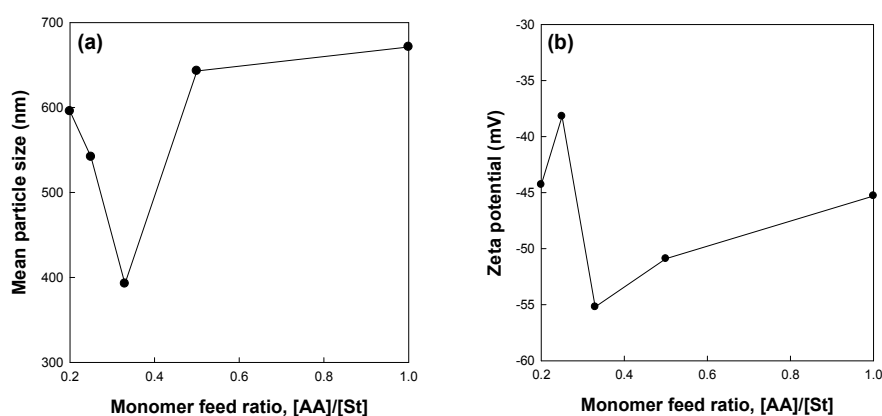


Figure 1. Effects of the monomer feed ratio on (a) mean particle size and (b) zeta potential of the St/AA submicroparticles prepared at 1.0×10^{-3} mol and 2.0×10^{-3} mol/mol of monomer for SDS and AIBN concentrations, respectively.

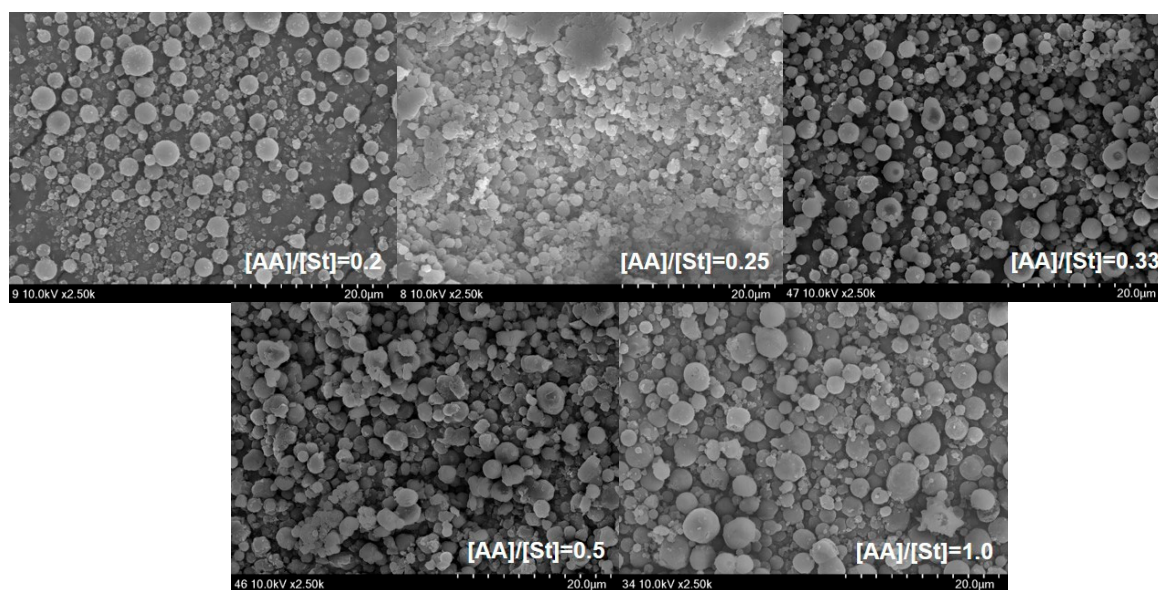


Figure 2. SEM photographs of St/AA submicrocapsules prepared at 1.0×10^{-3} mol and 2.0×10^{-3} mol/mol of monomer for SDS and AIBN concentrations, respectively, with a varying monomer feed ratio.

3.2. Effects of Surfactant Concentration

Figure 3 shows the effects of surfactant concentration on the mean particle size and zeta potential of St/AA submicrocapsules prepared at 0.33 and 2.0×10^{-3} mol/mol of monomer for [AA]/[St] and AIBN concentrations, respectively. The mean particle size of the submicrocapsules decreased with the increasing surfactant concentration (Figure 3a). This result is in good agreement with those of other researchers, suggesting that more SDS molecules are available for stabilizing the oil–water interfacial area generated during homogenization at a higher level of SDS [29,31–33]. The zeta potential of submicrocapsules, however, showed the optimum value at 1.0×10^{-3} mole of surfactant concentration (Figure 3b).

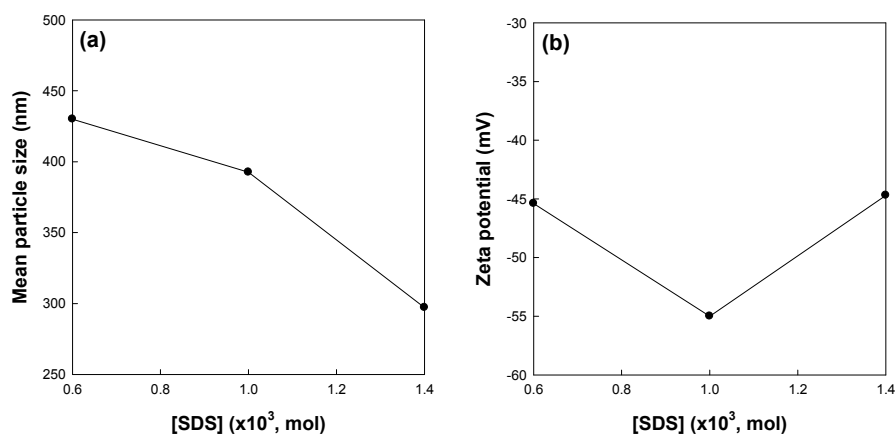


Figure 3. Effects of surfactant concentration on (a) mean particle size and (b) zeta potential of St/AA submicroparticles prepared at 0.33 and 2.0×10^{-3} mol/mol of monomer for [AA]/[St] and AIBN concentration, respectively.

Elimelech and O'Melia [34] reported that the collision efficiency of colloidal particles is independent of particle size. They also suggested that coupling of electrostatics and hydrodynamics, and the possible effects of surface roughness have a significant effect on the kinetics of particle–particle interaction. With the increase in the concentration of SDS, a large number of smaller micelles can be obtained. Therefore, St/AA submicrocapsules prepared from these micelles are supposed to have a relatively thin and low molecular weight electrostatic polyacrylic shell. This meager swollen layer will become vulnerable to aggregation and, as a result, show lower zeta potential. This reduction in the absolute value of zeta potential at higher SDS content can be confirmed by Figure 4 which presents SEM photographs of St/AA submicroparticles with varying surfactant concentrations.

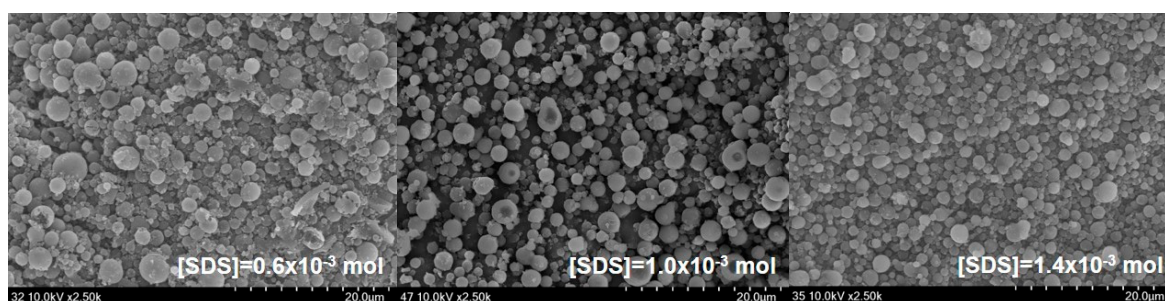


Figure 4. SEM photographs of St/AA submicroparticles prepared at 0.33 and 2.0×10^{-3} mol/mol of monomer for [AA]/[St] and AIBN concentration, respectively, with varying surfactant content.

3.3. Effects of Initiator Concentration

Figure 5 shows the effects of the initiator concentration on the mean particle size and zeta potential of St/AA submicrocapsules prepared at 0.33 and 1.0×10^{-3} mol for [AA]/[St] and SDS concentrations, respectively. As is well known, the initiator concentration greatly affects the reaction rate and extent of radical polymerization. The increase in initiator concentration at a fixed amount of surfactant will increase the possibility and frequency of droplet nucleation in a micelle. At this point, preference of AA for copolymerization with St is no longer maintained. Therefore, the hydrophilic swollen layer composed of longer polyacrylic blocks and the resulting zeta potential of St/AA submicrocapsules were assumed to be diminished for higher initiator concentrations. On the other hand, a limited amount of initiator could not properly activate the droplet nucleation. At an initiator concentration of 1.0×10^{-3} mol/mol of monomer, it was proposed that submicrocapsules were formed insufficiently, which was confirmed by large particle size and low zeta potential. As shown in Figure 5b, the St/AA

submicrocapsule prepared at 1.0×10^{-3} mol/mol of monomer of the initiator concentration shows no surface potential (almost zero potential) which means that immense coagulation of particles will occur.

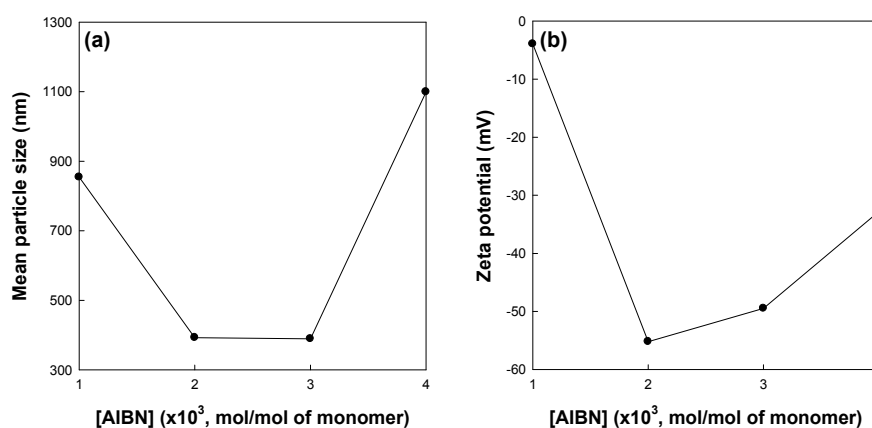


Figure 5. Effects of the initiator concentration on (a) mean particle size and (b) zeta potential of St/AA submicroparticles prepared at 0.33 and 1.0×10^{-3} mol for [AA]/[St] and SDS concentration, respectively.

3.4. Colloidal Stability

In this work, the long-term stability of St/AA submicrocapsules containing phytoncide oil was investigated by evaluating both the optical transmission and the photon backscattering profiles of the aqueous dispersion of submicrocapsules by using the TurbiscanTM Lab (Formulation, Toulouse, France) [35]. Measurements were carried out using a pulsed near infrared LED at a wavelength of 880 nm for 24 h. Two different synchronous optical sensors received the light transmitted through and backscattered by samples at an angle of 180° and 45° with respect to the incident radiation, respectively. Transmitted and backscattered light flux were correlated as a percentage to those of reference standards. If there was no variation greater than 2% in the backscattering profile, it can be considered as a stable formulation [36].

The transmission and backscattering profiles of the St/AA submicrocapsule aqueous dispersion prepared at the optimum condition ([AA]/[St] = 0.33; [SDS] = 1.0×10^{-3} mol; [AIBN] = 2.0×10^{-3} mol/mol of monomer) are shown in Figure 6. Variations of transmission and backscattering profiles were not correlated to the destabilization processes below the sample height of 5 mm and over that of 40 mm, the values having been determined by enclosed air in the bottom and/or on the top of the cylindrical glass tube, respectively. Analysis of the submicrocapsule dispersion showed that backscattering was the prevalent signal and there were almost no variations in the backscattering intensity for the entire test height. From this result, it can be confirmed that St/AA submicrocapsules prepared at the optimum condition could be formulated as stable colloids without aggregation.

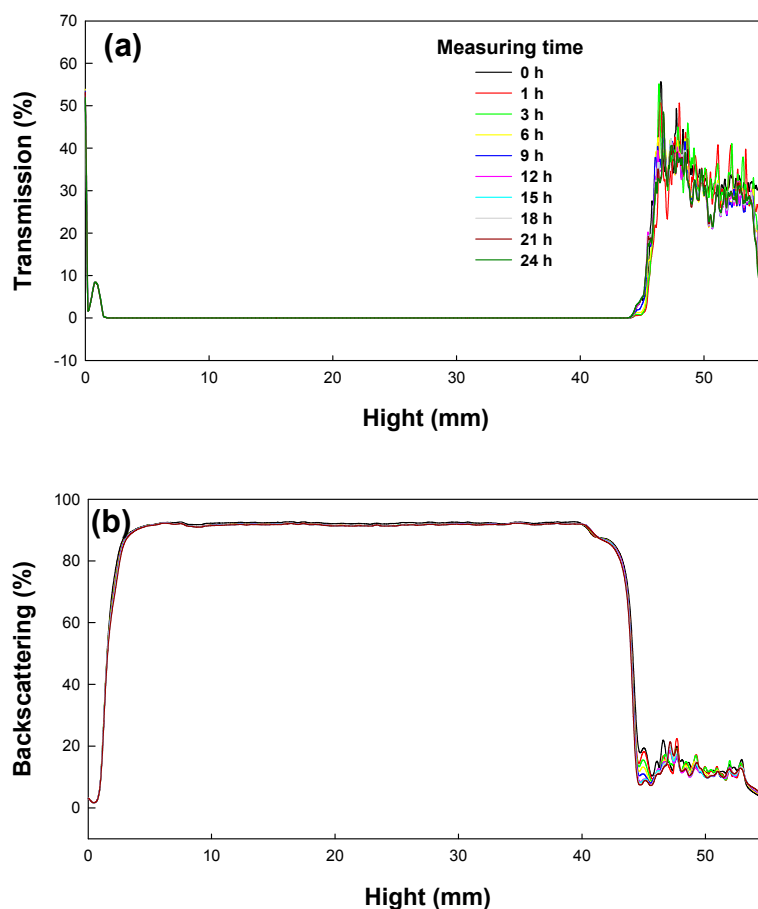


Figure 6. Transmission and backscattering profiles of St/AA submicrocapsule aqueous dispersion. (Prepared at the optimum miniemulsion condition of $[AA]/[St] = 0.33$, $[SDS] = 1.0 \times 10^{-3}$ mol, $[AIBN] = 2.0 \times 10^{-3}$ mol/mol of monomer).

4. Conclusions

It was shown that St/AA submicrocapsules can be obtained by miniemulsion copolymerization of AA and St with lyophobic core materials. There was an optimum condition for obtaining electronically stable St/AA submicrocapsules in the aqueous phase.

With the increase of $[AA]$, the mean particle size and zeta potential of St/AA submicrocapsules were greatly decreased due to anionic AA and polyacrylic blocks in micelles and submicrocapsules, respectively. However, at over $[AA]/[St] = 0.33$, the mean particle size of St/AA submicrocapsules was increased, which was ascribed to the particle agglomeration in the aqueous phase due to the increased hydrophilic swollen layer of the particles and the resulting reduction in surface area and zeta potential. The increase in the applied amount of surfactant assures the reduction in size of micelles and resulting St/AA submicrocapsules. At higher $[SDS]$ of over 1.0×10^{-3} mol, however, the formation of the weakened swollen layer, causing particle aggregation and a decrease in zeta potential, was suspected. Mean particle size and zeta potential of St/AA submicrocapsules were at the optimum condition at an initiator concentration of 2.0×10^{-3} mol/mol of monomer. Droplet nucleation was not effectively activated at a lower initiator concentration. At a higher initiator concentration, particle aggregation was manifested by virtue of the reduction in the portion of polyacrylic blocks in the swollen layer around the submicrocapsules.

From the above consideration, the optimum condition for miniemulsion copolymerization of St and AA was determined as follows; $[AA]/[St] = 0.33$, $[SDS] = 1.0 \times 10^{-3}$ mol, and $[AIBN] = 2.0 \times 10^{-3}$ mol/mol of monomer. Long-term colloidal stability was also evaluated for

the optimum condition of St/AA submicrocapsules by measuring the optical transmission and the photon backscattering profiles of the aqueous dispersion. It is shown that backscattering was the prevalent signal and there were almost no variations in backscattering intensity, which means that St/AA submicrocapsules prepared at the optimum condition have superior colloidal stability without aggregation and sedimentation. These electrically stable St/AA submicrocapsules can be applied to various fields such as a targeted and/or sustained release drug delivery system, emulsion templating of 3D objects, additives for polymeric resins, highly dispersive fiber finishing agent, and so on.

Acknowledgments: This work was supported by the Human Resource Training Program for Regional Innovation and Creativity through the Ministry of Education and the National Research Foundation of Korea (Grant No. 2015H1C1A1035576). This material was also based upon work supported by the Ministry of Trade, Industry & Energy (MOTIE, Korea) under Industrial Technology Innovation Program (Grant No. 10048877).

Author Contributions: Han Do Ghim conceived and designed the experiments; Yura Hwang performed the experiments; Han Do Ghim and Minkwan Kim analyzed the data and wrote the paper.

Conflicts of Interest: The authors declare no conflict of interest. The founding sponsors had no role in the design of the study; in the collection, analyses, or interpretation of data; in the writing of the manuscript, and in the decision to publish the results.

References

1. Pressly, E.D.; Rossin, R.; Hagooley, A.; Fukukawa, K.; Messmore, B.W.; Welch, M.J.; Wooley, K.L.; Lamm, M.S.; Hule, R.A.; Pochan, D.J.; et al. Structural Effects on the Biodistribution and Positron Emission Tomography (PET) Imaging of Well-Defined ^{64}Cu -Labeled Nanoparticles Comprised of Amphiphilic Block Graft Copolymers. *Biomacromolecules* **2007**, *8*, 3126–3134. [[CrossRef](#)] [[PubMed](#)]
2. Tan, W.B.; Zhang, Y. Multi-Functional Chitosan Nanoparticles Encapsulating Quantum Dots and Gd-DTPA as Imaging Probes for Bio-Applications. *J. Nanosci. Nanotechnol.* **2007**, *7*, 2389–2393. [[CrossRef](#)] [[PubMed](#)]
3. Morello, A.P.; Burrell, R.; Mathiowitz, E. Preparation and Characterization of Poly(methyl methacrylate)—Iron(III) Oxide Microparticles Using a Modified Solvent Evaporation Method. *J. Microencapsul.* **2007**, *24*, 476–491. [[CrossRef](#)] [[PubMed](#)]
4. Guo, J.; Yang, W.; Deng, Y.; Wang, C.; Fu, S. Organic-Dye-Coupled Magnetic Nanoparticles Encaged Inside Thermoresponsive PNIPAM Microcapsules. *Small* **2005**, *1*, 737–743. [[CrossRef](#)]
5. Sarmento, B.; Ribeiro, A.J.; Veiga, F.; Ferreira, D.C.; Neufeld, R.J. Insulin-Loaded Nanoparticles are Prepared by Alginate Iontropic Pre-Gelation Followed by Chitosan Polyelectrolyte Complexation. *J. Nanosci. Nanotechnol.* **2007**, *7*, 2833–2841. [[CrossRef](#)] [[PubMed](#)]
6. Gan, Q.; Wang, T. Chitosan Nanoparticle as Protein Delivery Carrier—Systematic Examination of Fabrication Conditions for Efficient Loading and Release. *Colloids Surf. B* **2007**, *59*, 24–34. [[CrossRef](#)] [[PubMed](#)]
7. Bayer, I.S.; Fragouli, D.; Martorana, P.J.; Martiradonna, L.; Cingolani, R.; Athanassiou, A. Solvent Resistant Superhydrophobic Films from Self-emulsifying Carnauba Wax–Alcohol Emulsions. *Soft Matter* **2011**, *7*, 7939–7943. [[CrossRef](#)]
8. Bayer, I.S.; Steele, A.; Martorana, P.J.; Loth, E. Fabrication of Superhydrophobic Polyurethane/Organoclay Nano-structured Composites from Cyclomethicone-in-water Emulsions. *Appl. Surf. Sci.* **2010**, *257*, 823–826. [[CrossRef](#)]
9. Zhang, H.; Cooper, A.I. Synthesis and Applications of Emulsion-templated Porous Materials. *Soft Matter* **2005**, *1*, 107–113. [[CrossRef](#)]
10. Landfester, K. The Generation of Nanoparticles in Miniemulsions. *Adv. Mater.* **2001**, *13*, 765–768. [[CrossRef](#)]
11. Jiang, S.; Sun, A.; Deng, J.; Yang, W.; Yu, Q. Synthesis of Sub-100 nm Nanoparticles by Emulsifier-free Emulsion Polymerization of α -Methylstyrene, Methyl Methacrylate and Acrylic Acid. *J. Macromol. Sci. A* **2011**, *48*, 846–850. [[CrossRef](#)]
12. Jung, Y.J.; Govindaiah, P.; Choi, S.W.; Cheong, I.W.; Kim, J. Morphology and Conducting Property of Ag/Poly(pyrrole) Composite Nanoparticles: Effect of Polymeric Stabilizers. *Synth. Met.* **2011**, *161*, 1991–1995. [[CrossRef](#)]
13. Lee, S.M.; Lee, S.J.; Kim, J.H.; Cheong, I.W. Synthesis of Polystyrene/Polythiophene Core/Shell Nanoparticles by Dual Initiation. *Polymer* **2011**, *52*, 4227–4234. [[CrossRef](#)]

14. Nitta, S.K.; Numata, K. Biopolymer-Based Nanoparticles for Drug/Gene Delivery and Tissue Engineering. *Int. J. Mol. Sci.* **2013**, *14*, 1629–1654. [[CrossRef](#)] [[PubMed](#)]
15. Quintanar-Guerrero, D.; Allemann, E.; Doelker, E.; Fessi, H. Preparation and Characterization of Nanocapsules from Preformed Polymers by a New Process Based on Emulsification–Diffusion Technique. *Pharm. Res.* **1988**, *15*, 1056–1062. [[CrossRef](#)]
16. Kwon, H.; Lee, J.; Choi, S.; Jang, Y.; Kim, J. Preparation of PLGA Nanoparticles Containing Estrogen by Emulsification–Diffusion Method. *Colloids Surf. A* **2001**, *182*, 123–130. [[CrossRef](#)]
17. Lee, S.M.; Yoo, E.S.; Ghim, H.D.; Lee, S.J. Alginate Nanohydrogels Prepared by Emulsification–Diffusion Method. *Macromol. Res.* **2009**, *17*, 168–173. [[CrossRef](#)]
18. Mason, T.G.; Wilking, J.N.; Meleson, K.; Chang, C.B.; Graves, S.M. Nanoemulsions: Formation, Structure, and Physical Properties. *J. Phys. Condens. Matter* **2006**, *18*, R635–R666. [[CrossRef](#)]
19. Hunter, R.J. *Zeta Potential in Colloid Science: Principles and Applications*; Academic Press: London, UK, 1988; pp. 4–7. ISBN 0-12-361960-2.
20. Mandzy, N.; Grulke, E.; Druffel, T. Breakage of TiO₂ Agglomerates in Electrostatically Stabilized Aqueous Dispersions. *Powder Technol.* **2005**, *160*, 121–126. [[CrossRef](#)]
21. Greenwood, R.; Kendall, K. Selection of Suitable Dispersants for Aqueous Suspensions of Zirconia and Titania Powders using Acoustophoresis. *J. Eur. Ceram. Soc.* **1999**, *19*, 479–488. [[CrossRef](#)]
22. Hanaor, D.; Michelazzi, M.; Leonelli, C.; Sorrell, C. The Effects of Carboxylic Acids on the Aqueous Dispersion and Electrophoretic Deposition of ZrO₂. *J. Eur. Ceram. Soc.* **2012**, *32*, 235–244. [[CrossRef](#)]
23. Hanaor, D.; Michelazzi, M.; Veronesi, P.; Leonelli, C.; Romagnoli, M.; Sorrell, C. Anodic Aqueous Electrophoretic Deposition of Titanium Dioxide using Carboxylic Acids as Dispersing Agents. *J. Eur. Ceram. Soc.* **2011**, *31*, 1041–1047. [[CrossRef](#)]
24. Pettersson, A.; Marino, G.; Pursiheimo, A.; Rosenholm, J. Electrosteric Stabilization of Al₂O₃, ZrO₂, and 3Y-ZrO₂ Suspensions: Effect of Dissociation and Type of Polyelectrolyte. *J. Colloid Interface Sci.* **2000**, *228*, 73–81. [[CrossRef](#)] [[PubMed](#)]
25. Han, M.; Lee, E.; Kim, E. Preparation and Optical Properties of Polystyrene Nanocapsules Containing Photochromophores. *Opt. Mater.* **2003**, *21*, 579–583. [[CrossRef](#)]
26. Fang, Y.; Yu, H.; Wan, W.; Gao, X.; Zhang, Z. Preparation and Thermal Performance of Polystyrene/*n*-Tetradecane Composite Nanoencapsulated Cold Energy Storage Phase Change Materials. *Energy Convers. Manag.* **2013**, *76*, 430–436. [[CrossRef](#)]
27. Wang, P.H.; Pan, C. Preparation of Styrene/Acrylic acid Copolymer Microspheres: Polymerization Mechanism and Carboxyl Group Distribution. *Colloid Polym. Sci.* **2002**, *280*, 152–159. [[CrossRef](#)]
28. Musyanovych, A.; Rossmannith, R.; Tontsch, C.; Landfester, K. Effect of Hydrophilic Comonomer and Surfactant Type on the Colloidal Stability and Size Distribution of Carboxyl- and Amino-Functionalized Polystyrene Particles Prepared by Miniemulsion Polymerization. *Langmuir* **2007**, *23*, 5367–5376. [[CrossRef](#)] [[PubMed](#)]
29. Holzapfel, V.; Musyanovych, A.; Landfester, K.; Lorenz, M.R.; Mailander, V. Preparation of Fluorescent Carboxyl and Amino Functionalized Polystyrene Particles by Miniemulsion Polymerization as Markers for Cells. *Macromol. Chem. Phys.* **2005**, *206*, 2440–2449. [[CrossRef](#)]
30. Kim, S.H.; Kim, B.J.; Kwon, D.I.; Park, K.H. Preparation of Polystyrene Particles Containing Poly(ethylene glyco) Groups and Their Surface Charge Characterization in Dielectric Medium. *Polymer* **2004**, *28*, 524–530.
31. Kim, B.; Oh, S.; Han, M.; Im, S. Synthesis and Characterization of Polyaniline Nanoparticles in SDS Micellar Solutions. *Synth. Met.* **2001**, *122*, 297–304. [[CrossRef](#)]
32. Li, Y.; Xiao, W.; Xiao, K.; Berti, L.; Luo, J.; Tseng, H.P.; Fung, G.; Lam, K.S. Well-Defined, Reversible Boronate Crosslinked Nanocarriers for Targeted Drug Delivery in Response to Acidic pH Values and cis-Diols. *Angew. Chem.* **2012**, *124*, 2918–2923. [[CrossRef](#)]
33. Preuss, M.; Butt, H. Direct Measurement of Particle–Bubble Interactions in Aqueous Electrolyte: Dependence on Surfactant. *Langmuir* **1998**, *14*, 3164–3174. [[CrossRef](#)]
34. Elimelech, M.; O'Melia, C.R. Effect of Particle Size on Collision Efficiency in the Deposition of Brownian Particles with Electrostatic Energy Barriers. *Langmuir* **1990**, *6*, 1153–1163. [[CrossRef](#)]

35. Menguala, O.; Meuniera, G.; Cayrea, I.; Puecha, K.; Snabreb, P. Characterisation of Instability of Concentrated Dispersions by a New Optical Analyser: The Turbiscan MA 1000. *Colloids Surf. A* **1999**, *152*, 111–123. [[CrossRef](#)]
36. Celia, C.; Trapasso, E.; Cosco, D.; Paolino, D.; Fresta, M. Turbiscan Lab[®] Expert Analysis of the Stability of Ethosomes[®] and Ultradeformable Liposomes Containing a Bilayer Fluidizing Agent. *Colloids Surf. B* **2009**, *72*, 155–160. [[CrossRef](#)] [[PubMed](#)]



© 2017 by the authors. Licensee MDPI, Basel, Switzerland. This article is an open access article distributed under the terms and conditions of the Creative Commons Attribution (CC BY) license (<http://creativecommons.org/licenses/by/4.0/>).